JACS
JOURNAL OF THE AMERICAN CHEMICAL SOCIETY
Article
pubs.acs.org/JACS

Synthesis and Characterization of [*n*]CPP (*n* = 5, 6, 8, 10, and 12) Radical Cation and Dications: Size-Dependent Absorption, Spin, and Charge Delocalization

Eiichi Kayahara,[†,§] Takahiko Kouyama,[#] Tatsuhisa Kato,[#,‡] and Shigeru Yamago*[,†,§]

[†]Institute for Chemical Research, Kyoto University, Uji 611-0011, Japan
[§]Core Research for Evolutional Science and Technology (CREST), Japan Science and Technology Agency, Tokyo 102-0076, Japan
[#]Graduate School of Human and Environmental Sciences, Kyoto University, Sakyo-ku, Kyoto 606-8501, Japan
[‡]Institute for Liberal Arts and Sciences, Kyoto University, Sakyo-ku, Kyoto 606-8501, Japan

Supporting Information

ABSTRACT: Radical cations and dications of [*n*]cyclo-*p*-phenylenes ([*n*]CPPs, *n* = 5, 6, 10, and 12), which are the models of those of linear oligo-*p*-phenylenes without a terminus, were synthesized as hexafluoroantimonate salts by the one- and two-electron chemical oxidation of CPP by $NOSbF_6$ or SbF_5. The radical cations, [*n*]$CPP^{\bullet+}$, and dications, [*n*]CPP^{2+}, exhibited remarkable bathochromic shifts in their UV−vis−NIR absorption bands, suggesting that [*n*]$CPP^{\bullet+}$ and larger [*n*]CPP^{2+} exhibit longer polyene character than the shorter analogues. The larger bathochromic shift was consistent with the narrower HOMO−SOMO and HOMO−LUMO gaps in larger [*n*]$CPP^{\bullet+}$ and [*n*]CPP^{2+}, respectively. In [*n*]$CPP^{\bullet+}$, the spins and charges were equally and fully delocalized over the *p*-phenylene rings of the CPPs, as noted by ESR. ^{1}H NMR revealed that the hydrogen of [*n*]CPP^{2+} shifted to a high magnetic field from the neutral compounds due to the diamagnetic ring current derived from the in-plane aromaticity of [*n*]CPP^{2+}. The single resonances observed in all [*n*]CPP^{2+} strongly suggest the complete delocalization of the charges over the CPPs. Furthermore, the contribution of biradical character was clarified for [10]- and [12]CPP by VT-NMR experiment and theoretical calculation.

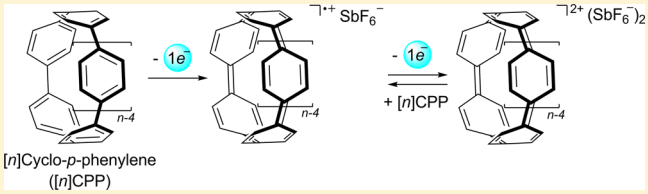

INTRODUCTION

Radical cations and dications of π-conjugated oligomers and polymers play a decisive role in charge transfer and migration in organic electronic devices, such as organic light-emitting diodes, organic semiconductors, organic photovoltaics, and molecular electronic wires.[1−9] Their structure and the delocalization or localization of charge and spin have garnered considerable attention in regard to the mechanism of charge transport. While significant progress has been made in isolating and characterizing π-radical cations and dications of oligomers with well-defined structures to address these issues,[10−15] the majority of the products has been heteroatom-stabilized compounds, and the spin and charge (de)localization was perturbed by the heteroatoms. The only exception was the radical cation of oligo-*p*-phenylenes reported by Rathore and co-workers.[16,17] However, while the positive charge was somewhat delocalized over all phenylene moieties, as judged by absorption, it was more localized in the middle of the oligomers, even in the quaterphenyl compound. While the results were rationalized by the existence of a terminal structure, conclusive evidence was not provided.

Recently, cyclo-*p*-phenylenes (CPPs, Chart 1a), which belong to a new class of conjugated oligomers that constitute the cyclic version of oligo-*p*-phenylenes without a terminus, have garnered considerable attention.[18−24] As a result of recent advances in synthetic studies of CPPs[25−47] and their analogues,[48−67] various unique physical properties of CPPs, such as size-dependent redox[42,44,45,68−72] and photophysical properties[73−80] and size-complementary host−guest chemistry,[81−85] have been revealed. Notably, redox properties are closely associated with charge delocalization in π-conjugated oligomers and polymers. For example, we recently reported that [5]-[13]CPPs undergo reversible oxidation reactions, as revealed by electrochemical analyses.[42,44,45] Furthermore, we recently reported that [8]$CPP^{\bullet+}SbF_6^-$ (Chart 1b) and the

Chart 1. Structure of (a) [*n*]CPP, (b) [*n*]CPP Radical Cation, and (c) [*n*]CPP Dication

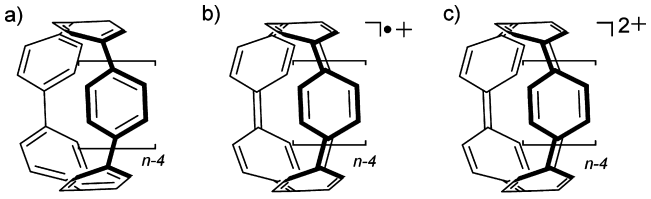

Received: October 22, 2015
Published: December 17, 2015

DOI: 10.1021/jacs.5b10855
J. Am. Chem. Soc. 2016, 138, 338−344

dication [8]CPP^{2+}(SbF_6^-)$_2$ (Chart 1c) could be prepared by the chemical oxidation of [8]CPP and isolated in pure form.[68,71] All spectroscopic analyses and theoretical studies revealed that, in sharp contrast to the results of Rathore,[16,17] the spin and charge were fully delocalized over all eight *p*-phenylene units. The results posed a new question regarding the delocalization of spin and charge in CPPs: Over how many *p*-phenylene units can the charge and spin be localized?

Here, we report the selective synthesis and characterization of [*n*]CPP (*n* = 5, 6, 10, 12) radical cations and dications by the chemical oxidation of [*n*]CPPs. The absorption spectra of the compounds were highly sensitive to ring size, and larger CPP radical cations and dications exhibited absorptions at longer wavelengths, suggesting the existence of longer conjugation. In addition, the spin and charge were completely delocalized over all *p*-phenylene units in all CPP radical cations and dications, as assessed by electron spin resonance (ESR) and ^{1}H NMR, while the contribution of diradical character is also suggested for the larger CPPs by ^{1}H NMR. The radical cation and dication of [12]CPP possess the longest conjugation and delocalization among those of π-conjugated oligomers so far reported, and the results clearly suggest that the spin and charge can be delocalized more than 12 *p*-phenylene units in oligo- and poly-*p*-phenylenes.

RESULTS AND DISCUSSION

Synthesis and Isolation of [*n*]CPP Radical Cations and Dications. The chemical oxidation of [*n*]CPPs (*n* = 5, 6, 10, and 12) was carried out (Scheme 1) using a procedure similar

Scheme 1. Synthesis of [*n*]CPP Radical Cations and Dications

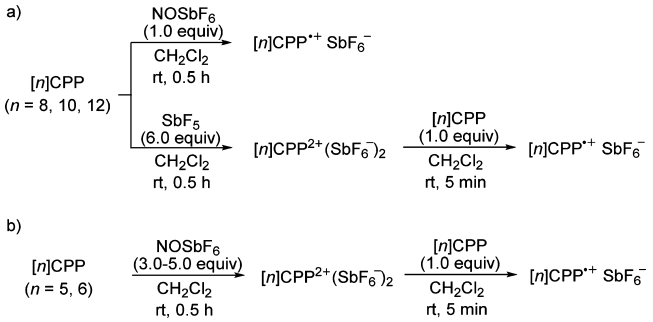

to that used for the synthesis of [8]CPP radical cation and dications,[68] where nitrosonium hexafluoroantimonate ($NOSbF_6$) was used as an oxidant.[86] [10]- and [12]CPPs were selectively converted to the corresponding the radical cations by employing 1.0 equiv of $NOSbF_6$ in CH_2Cl_2 at room temperature; the radical cation salts, [10]- and [12]CPP$^{\bullet+}$-SbF_6^-, were isolated as purple and black-green solids in 61 and 78% yield, respectively (Scheme 1a). However, $NOSbF_6$ could not fully convert the CPPs to the corresponding dications even when an excess was used. This was probably because the HOMO energies of [10]- and [12]CPP are lower than that of [8]CPP;[42] thus, larger CPPs are more resistant to oxidation than [8]CPP. SbF_5, which is a more powerful oxidizing agent than $NOSbF_6$, was effective and gave the corresponding dications, [10]- and [12]CPP^{2+}(SbF_6^-)$_2$ in 80 and 87% yield as green and black solids, respectively. The reaction of the dications and corresponding neutral CPPs led to the quantitative formation of the radical cations.

The oxidation of [5]CPP with 1.0 equiv of $NOSbF_6$ in CH_2Cl_2 at room temperature, on the other hand, resulted in a mixture of the radical cation and dication in a 1:4 ratio, as judged by UV−vis spectroscopy. However, the dication, [5]CPP^{2+}(SbF_6^-)$_2$, formed selectively and was isolated in 92% yield as a green solid upon treatment of [5]CPP with excess (3.0 equiv) of $NOSbF_6$ (Scheme 1b). Furthermore, the reaction between the dication and neutral [5]CPP (1.0 equiv) gave the radical cation, [5]CPP$^{\bullet+}SbF_6^-$, as a brown solid in 74% yield.

The dication of [6]CPP, [6]CPP^{2+}(SbF_6^-)$_2$, was also isolated in a high yield as a reddish purple solid upon oxidation with excess $NOSbF_6$. Furthermore, the radical cation, [6]CPP$^{\bullet+}$-SbF_6^-, was also prepared in high yield as a black green solid upon reaction of the dication and neutral [6]CPP, even though the selective single-electron oxidation of neutral [6]CPP by $NOSbF_6$ was not successful.

The stability of the radical cations depended on the size of CPPs, while that of the dication was insensitive to the size. For the radical cations, [5] and [6]CPP$^{\bullet+}SbF_6$ as well as [8]CPP$^{\bullet+}SbF_6$ were stable under nitrogen and were stored at −30 °C for more than 3 months, while they decomposed within 12 h at room temperature when exposed to air. On the contrary, [10]- and [12]CPP radical cations easily disproportionated to the corresponding dication and neutral CPP within 2 h at room temperature. The origin of the instability is unclear at this moment and needs further studies to clarify this point. On the other hand, all dications were remarkably stable under nitrogen and no apparent decomposition was observed at −30 °C even after 6 months; the stability is consistent with the existence of in-plane aromaticity in the CPP dications. Nevertheless, they decomposed within 1 day at room temperature upon exposure to air.

UV−Vis−Near-Infrared (NIR) Spectra of [*n*]CPP Radical Cation and Dication. UV−vis−NIR spectra of the radical cations and dications were measured in CH_2Cl_2 (Figure 1), and the absorption maxima (λ_{max}) are summarized in Table 1. All CPP radical cations and dications exhibited a large bathochromic shift in the maximum absorption relative to those of the neutral CPPs. For example, a solution of [5]CPP$^{\bullet+}SbF_6^-$ showed a characteristic broad absorption band that extended to the NIR region (λ_{max} = 876 nm) together with several broad absorption bands in the visible region, whereas neutral [5]CPP exhibited intense absorption bands at λ_{max} = 350 nm. Two distinct absorptions bands at λ_{max} = 654 nm and λ_{max} = 428 nm were observed for the dication, [5]CPP^{2+}(SbF_6^-)$_2$.

Significant size dependence was observed for the radical cations and dications; larger CPPs absorbed at longer wavelengths. For example, the λ_{max} of the [6]-, [8]-, and [10]CPP radical cations shifted from 340 nm of the neutral compounds to 1136, 1770, and 2110 nm, respectively. Furthermore, the λ_{max} exceeded 2700 nm for [12]CPP. For the dications, the λ_{max} of the low-energy absorption of [5]-, [6]-, [8]-, [10]-, and [12]CPPs shifted to 654, 792, 1102, 1568, and 2109 nm, respectively, and the λ_{max} of the high-energy absorption increased from 428 to 600 nm for [5]- to [12]CPPs.

The transition energies ($E = hc/\lambda_{max}$) of the NIR bands for the radical cations and the lowest-energy absorption for the dications were plotted against the reciprocal number of *p*-phenylene units (1/*n*) (Figure 2). In both cases, excellent linear correlations were observed, which strongly suggest the effective π-conjugation over the *p*-phenylene units in all cases.

DOI: 10.1021/jacs.5b10855
J. Am. Chem. Soc. 2016, 138, 338−344

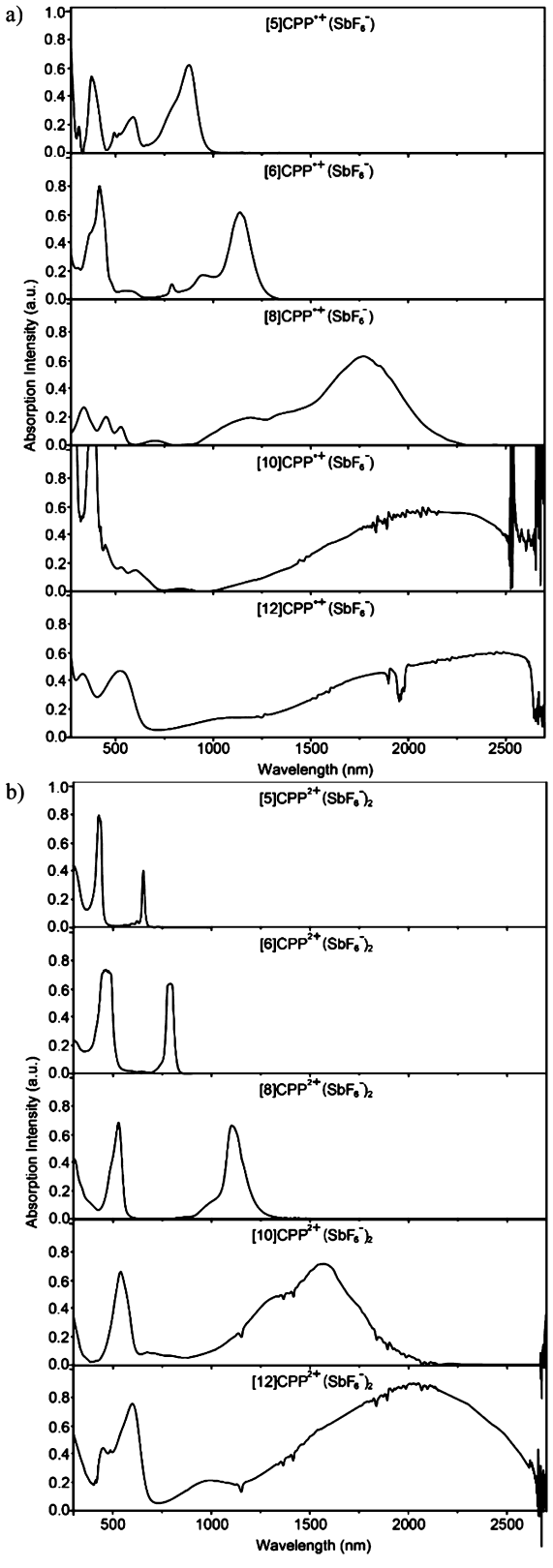

Figure 1. UV−vis−NIR spectra of (a) $[n]CPP^{\bullet+}SbF_6^-$ and (b) $[n]CPP^{2+}(SbF_6^-)_2$ in CH_2Cl_2 (1×10^{-4} mol L^{-1}) at 25 °C.

The absorption bands of the radical cations and dications were characterized using time-dependent density functional theory (TD-DFT) calculations at the (U)B3LYP/6-31G(d) level of theory (Table 1). For all radical cations, broad absorptions in the NIR region were assigned as the transition from the nearly degenerate HOMOs to the SOMO. For the dications, low- and high-energy absorption bands were assigned to the transition from the nearly degenerate HOMOs to the LUMO and the degenerate HOMOs to the LUMO+1. The assignments were consistent with our previous works.[68,70,71] The calculated λ_{max} shifted bathochromically as the ring size increased. The plot of the transition energy obtained from the calculated λ_{max} values against $1/n$ showed good linear correlations (Figure 2). The results were almost identical to the experimental results but in good contrast to the UV absorption maximum of neutral CPPs, which is insensitive to ring size (see below).

To gain insights into the size dependence of the transition energies of the radical cations and the dications, molecular orbital (MO) analysis was carried out. The most stable isomer was used for the analysis (Table S2), while several rotational isomers with close energy were located. Similar to neutral CPPs, the most stable isomer of the radical cation and dication for a CPP having even *p*-phenylene units possess an alternating zigzag orientation of *p*-phenylene units with nearly $D_{(n/2)d}$ point group symmetry, and that of an odd CPP have C_1 point group symmetry having a helical arrangement of the PP units.

As previously reported,[42] the HOMO and LUMO energies of neutral CPPs become higher and lower as the decrease of ring size because of the strain-induced increase of the quinoidal contribution (Figure 3a). However, the HOMO/LUMO transition is forbidden, and the maximum absorption of all neutral CPPs corresponds to the sum of the nearly degenerated HOMO−2 and HOMO−1 to LUMO, and the HOMO to the nearly degenerated LUMO+1 and LUMO+2 transitions.

Table 1. Photophysical Properties of $[n]CPP^{\bullet+}$ SbF_6^- and $[n]CPP^{2+}$ $(SbF_6^-)_2$

	λ_{max} (nm), [exptl (calcd[a])]		
n	[*n*]CPP	$[n]CPP^{\bullet+}(SbF_6^-)$	$[n]CPP^{2+}(SbF_6^-)_2$
5	338 (340)	876 (758)	654, 428 (603, 382)
6	341 (340)	1136 (976)	792, 464 (705, 405)
8	344 (340)	1770 (1413)	1102, 528 (923, 429)
10	343 (340)	2110 (1843)	1568, 549 (1156, 430)
12	344 (352)	>2700 (2268)	2109, 600 (1607, 430)

[a]Obtained by TD-DFT calculations at the (U)B3LYP/6-31G* level of theory.

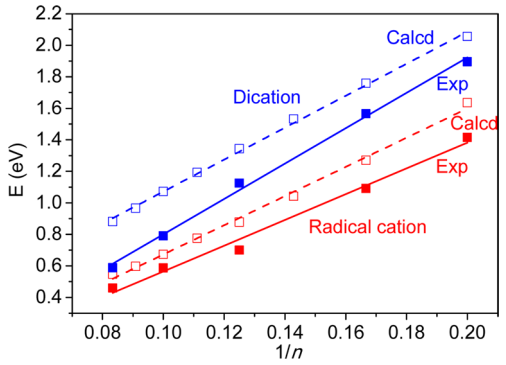

Figure 2. Plots of transition energies against reciprocal number ($1/n$) of [*n*]CPPs for the radical cations (red) and dications (blue). Filled and open squares represent the experimental and theoretical data, respectively.

DOI: 10.1021/jacs.5b10855
J. Am. Chem. Soc. 2016, 138, 338−344

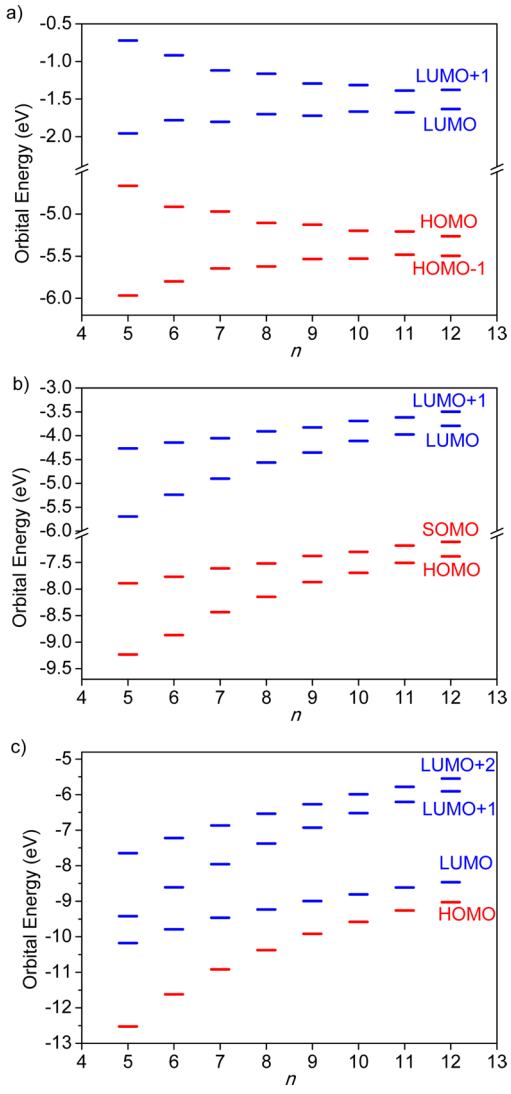

Figure 3. Orbital energies for a) [*n*]CPP, b) [*n*]CPP$^{\bullet+}$, and c) [*n*]CPP^{2+} obtained from DFT calculations at the (U)B3LYP/6-31G(d) level of theory.

Because their orbital energy gaps are insensitive to size, the maximum absorption of neutral CPPs is insensitive to the size.

For the radical cations, the energies of HOMO, SOMO, LUMO, and LUMO+1 increased as the ring size increased (Figure 3b). Notably, the HOMO and LUMO energies were more sensitive to ring size than the SOMO energies. As a result, the SOMO/HOMO gaps became smaller in larger CPP radical cations, which lead to larger bathochromic shifts in the NIR absorption bands. As previously reported,[70] the HOMO, SOMO, LUMOs, and LUMO+1 of the radial cations were derived from HOMO−1, HOMO, LUMOs, and LUMO+1 of neutral CPPs, respectively. Thus, the observed size-dependence of the NIR absorption bands of the radical cations was reflected by the size-dependence of the HOMO−1/HOMO gaps of the neutral CPPs. The SOMO energy increases as increasing the size, and the size-dependence is different from the HOMO of neutral CPPs, but the difference would be due to increase of the in-plane conjugation in the radical cations so that the larger radical cations have longer conjugation length.

Similar discussion could be applied to the dications, and the LUMO and HOMO of the dications are derived from the SOMO and HOMO of the radical cation and HOMO and HOMO−1 of neutral CPPs, respectively. The energies of the degenerated HOMO, LUMO, LUMO+1, and LUMO+2 increased as the ring size increased (Figure 3c); the increase in the HOMO and LUMO+1 energies was larger than that of the other orbital energies. Thus, in large CPP dications, the HOMO/LUMO gap became narrower, and a larger bathochromic shift in the absorption bands occurred.

ESR Spectra. All CPP radical cations were ESR active and ^{1}H NMR silent, which was consistent with the formation of paramagnetic species. The ESR spectra of CPP$^{\bullet+}$ in CH_2Cl_2 solution (1.0×10^{-3} mol L^{-1}) at 25 °C, as shown as a red line in Figure 4, showed an equally split multiplet in all cases,

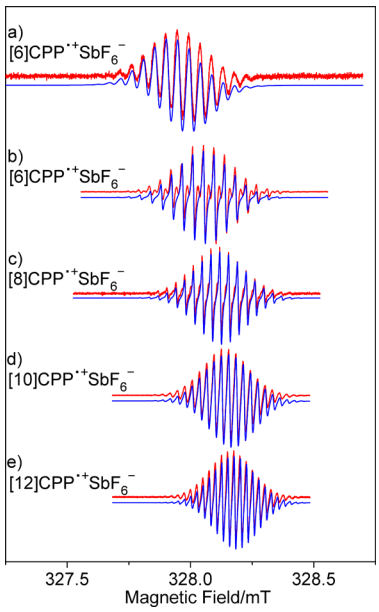

Figure 4. ESR spectra of [*n*]CPP$^{\bullet+}$SbF$_6^-$ in CH_2Cl_2 (1×10^{-3} mol L^{-1}) at 25 °C. Red and blue lines represent observed and simulated spectra, respectively.

suggesting that the spin was equally delocalized over all *p*-phenylene units in all cases. The simulated spectra (blue line in Figure 4) assuming that all hydrogen atoms are chemically equivalent could be superimposed with the observed spectra in all cases, clearly suggesting that the spin was completely delocalized over all *p*-phenylene units in the radical cations. The ^{1}H hyperfine coupling constants (hfcc's) of [5]-, [6]-, [8]-, [10]-, and [12]CPP radical cations were 0.046, 0.0429, 0.0343, 0.0293, and 0.0249 mT, respectively. Furthermore, when the ^{1}H hfcc was plotted against the reciprocal number of *p*-phenylene units ($1/n$), a good linear correlation (R^2 = 0.98) was observed, and the result is consistent with the fully delocalization of the spin. The relationship could also be reproduced from the ^{1}H hfcc obtained by DFT calculations (Figure 5). The *g* values of [5]-, [6]-, [8]-, [10]-, and [12]CPP radical cations were found to be 2.0043, 2.0037, 2.0033, 2.0031, and 2.0030, respectively. All cation radicals exhibited values bigger than that of the free electron (2.0023). This positive *g* shift indicated that [*n*]CPP$^{\bullet+}$ had a low-lying excited state characterized by a hole-promoted configuration. The different deviations from g = 2.0023 were due to the position of the low-lying excited state.[87−89]

DOI: 10.1021/jacs.5b10855
J. Am. Chem. Soc. 2016, 138, 338−344

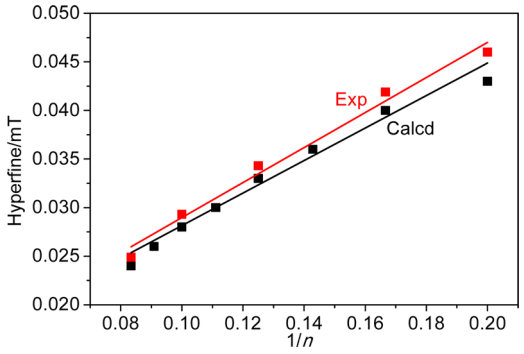

Figure 5. Correlation between ^{1}H hyperfine coupling constants and reciprocal number of repeating *p*-phenylene units ($1/n$) of [*n*]CPP$^{\bullet+}$-SbF_6^-. Red and black colors represent experimental and theoretical data, respectively.

Calculations of charge and spin density on [*n*]CPP$^{\bullet+}$ (*n* = 5−12) provided further evidence for the spin delocalization. The Mulliken analysis of all radical cations clearly demonstrated that the spin and positive charge were fully delocalized over all phenylene units (Table S6, Figure S17). In each phenylene unit, the computed Mulliken atomic charges (and spin densities) on the ipso carbon atoms were about +0.10 (and 0.07−0.03), whereas those on the ortho carbon atoms were about −0.17 (0.014−0.006). For [*n*]CPP^{2+}, the charges on the ipso and ortho carbon atoms were about +0.105 and −0.15 to −0.17, respectively. Thus, the spin density of the ipso carbon was higher than that of the ortho carbon, while the charge was more equally distributed between the ipso and ortho carbon atoms. Furthermore, the spin density and charge of the ortho carbon atoms were slightly different, but they could be averaged on the ESR time scale.

NMR Study of Dications. All dications showed well-resolved peaks in the ^{1}H NMR spectra in CD_2Cl_2 at room temperature (Figure 6 and Table 2). For [10]- and [12]CPP dications, peak intensity was weaker than that of smaller dications and the peak broadening was observed. This observation should suggest the contribution of biradical species (see below). Despite its contribution, singlet signals observed for all CPP dications indicated the highly symmetrical structure of the dications on the NMR time scale. Furthermore, the signals appeared in the range of 4.5−5.5 ppm, which was upfield shifted as compared to those of neutral CPPs, which are worth mentioning because protons attached to an electron deficient carbon usually resonate at lower magnetic fields. The upfield shifts could be ascribed to the existence of strong magnetic desealing effects, owing to the in-plane aromaticity of the dications.[71] Furthermore, the chemical shift depended on the size of the ring and shifted upfield with increasing ring size, reaching 4.57 ppm for [12]CPP^{2+}. All these results are consistent with the delocalization of the cationic charges to all parapenylene units.

Gauge-independent atomic orbital (GIAO) calculations suggest that the protons directing to inside and outside of the center of a CPP ring, which are derive from the zigzag conformation of *p*-phenylene units, were magnetically non-equivalent (Table S2), and the inside protons were shifted upfield in all dications due to the in-plane aromaticity. No clear size dependence was observed for the nonequivalent GIAO values among [5]- to [12]CPP dications, and further studies are needed to clarify this point.

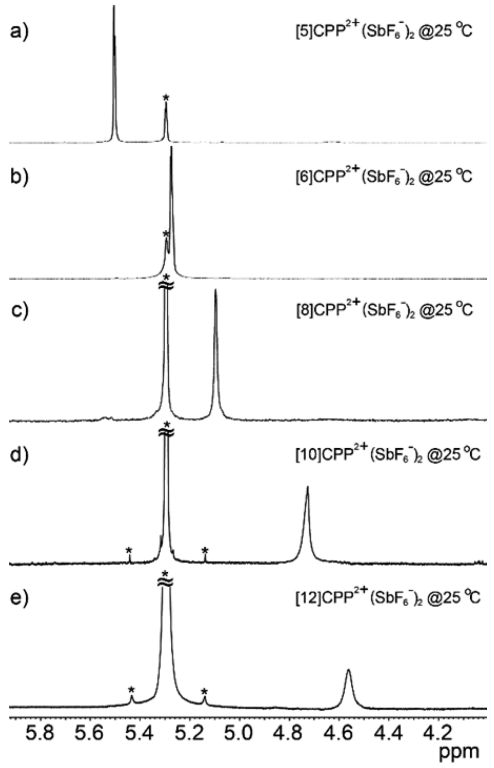

Figure 6. ^{1}H NMR spectra of [*n*]CPP^{2+}(SbF_6^-)$_2$ in CD_2Cl_2 at 25 °C. The peak of CH_2Cl_2 is marked.

Table 2. Summary of ^{1}H NMR Data and Average NICS Values (ppm) for [*n*]CPP Dications

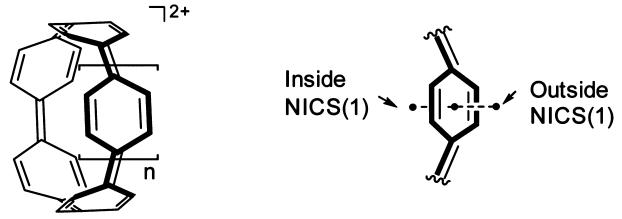

	^{1}H NMR (ppm)			NICS(1) (ppm)
n	exptl[a]	GIAO (average)[b]	GIAO (inside, outside)[b]	inside, outside[b,c]
5	5.53	4.94	4.90, 4.98	−28.6, −6.1
6	5.30	4.56	4.53, 4.58	−29.6, −5.5
7		4.39	3.21, 5.55	−29.3, −5.0
8	5.24	4.42	2.61, 6.25	−28.6, −4.7
9		4.54	2.17, 6.91	−25.7, −4.1
10	4.72	4.74	2.42, 7.08	−26.0, −4.4
11		4.89	1.79, 7.98	−24.8, −4.4
12	4.57	5.07	2.63, 7.53	−23.9, −4.4

[a]Measured in CD_2Cl_2 at 25 °C. [b]Determined using GIAO calculations of the geometry-optimized structures obtained at the B3LYP/6-31G* level of theory. [c]Averaged value.

The calculated nucleus-independent chemical shift (NICS) (1) values are negative for both the inside and outside of the hoop and the inside is more negative than the outside. Furthermore, the values became less negative with an increase in the number of *p*-phenylene units. In other words, larger dications had stronger polyene characteristics due to the stronger in-plane aromaticity. These results were consistent with the size dependence of the ^{1}H NMR chemical shift and

DOI: 10.1021/jacs.5b10855
J. Am. Chem. Soc. 2016, 138, 338−344

that of the UV−vis−NIR spectra, which showed a larger bathochromic shift in the absorption derived from the HOMO−LUMO transition in larger CPP dications. As a result, the larger dications could more efficiently expand their conjugation networks.

Finally, variable-temperature NMR spectroscopy was carried out to obtain the direct experimental evidence of biradical character in larger CPP dications. In the spectra of [10]CPP dication in CD_2Cl_4, the signal intensities increased by cooling from 25 °C to −15 °C, while further cooling did not cause any change (Figure S19). In contrast, the signal broadening occurred at high temperature, and the signal completely disappeared at 65 °C. The change of signal intensity was completely reversible both for low and high temperature. The same temperature dependence of peak intensity was observed for [12]CPP dication. On the contrary, [8]CPP dication did not show the change of peak intensity even heating at 80 °C. In addition, ESR spectra of [10]- and [12]CPP dications at 25 °C showed the signals with an equally split multiplet (Figure S22). These observations suggest the contribution of thermally excited triplet biradical species for larger CPP dication. The contribution of biradical at 25 °C was determined to be 37 and 72% for [10]- and [12]CPP dications, respectively, from the integration of NMR spectra (Figures S19−21).

Calculations provided further evidence for biradical character in larger CPP dications. Structure optimization of $[10]CPP^{2+}$ under unrestricted DFT method resulted in a structure having nearly C_2 point group symmetry as the most stable isomers (Table S2). In this structure, the spin density is not equally delocalized over all phenylene units but is largely localized at either end of a CPP ring (Figure S18, Table S10). Same spin localization was also made for [9]-, [11]-, and [12]CPP dications but not for smaller CPPs than [8]CPP. The results are consistent with the experimental observation.

SUMMARY

The radical cations and dications of [*n*]CPPs (*n* = 5, 6, 10, 12) were isolated by the one- and two-electron chemical oxidation of [*n*]CPP with $NOSbF_6$ or SbF_5. Both oxidized species showed a remarkable bathochromic shift in the absorption bands relative to those of the neutral [*n*]CPPs, and the size-dependence suggested more effective conjugation of the in-plane π-system in larger oxidized species. The spin and charges in the oxidized species were fully delocalized over the entire *p*-phenylene rings in the time scale of ESR and NMR measurement. These results also suggest efficient conjugation of the π-system in larger CPP dications, which was consistent with the UV−vis−NIR spectra. Furthermore, contribution of biradical character in the dications was clarified for the first time. These findings will aid in the understanding of charge and spin in doped conjugated oligomers and polymers, and in the design of π-electron materials for molecular electronics.

ASSOCIATED CONTENT

Supporting Information

The Supporting Information is available free of charge on the ACS Publications website at DOI: 10.1021/jacs.5b10855.

Synthesis and characterization of all new compounds, electrochemical analysis, and results of DFT calculations (PDF)

AUTHOR INFORMATION

Corresponding Author

*yamago@scl.kyoto-u.ac.jp

Notes

The authors declare no competing financial interest.

ACKNOWLEDGMENTS

This work was partly supported by the CREST Program of the Japan Science and Technology Agency (S.Y.) and by JSPS KAKENHI Grant No. 26410043 (E.K.).

REFERENCES

(1) Bredas, J. L.; Street, G. B. *Acc. Chem. Res.* **1985**, *18*, 309.
(2) Patil, A. O.; Heeger, A. J.; Wudl, F. *Chem. Rev.* **1988**, *88*, 183.
(3) Tolbert, L. M. *Acc. Chem. Res.* **1992**, *25*, 561.
(4) Martin, R. E.; Diederich, F. *Angew. Chem., Int. Ed.* **1999**, *38*, 1350.
(5) Watson, M. D.; Fechtenkötter, A.; Müllen, K. *Chem. Rev.* **2001**, *101*, 1267.
(6) Bendikov, M.; Wudl, F.; Perepichka, D. F. *Chem. Rev.* **2004**, *104*, 4891.
(7) Anthony, J. E. *Chem. Rev.* **2006**, *106*, 5028.
(8) Grimsdale, A. C.; Leok Chan, K.; Martin, R. E.; Jokisz, P. G.; Holmes, A. B. *Chem. Rev.* **2009**, *109*, 897.
(9) Heinze, J.; Frontana-Uribe, B. A.; Ludwigs, S. *Chem. Rev.* **2010**, *110*, 4724.
(10) Nishinaga, T.; Komatsu, K. *Org. Biomol. Chem.* **2005**, *3*, 561.
(11) Nishinaga, T.; Wakamiya, A.; Yamazaki, D.; Komatsu, K. *J. Am. Chem. Soc.* **2004**, *126*, 3163.
(12) Yamazaki, D.; Nishinaga, T.; Tanino, N.; Komatsu, K. *J. Am. Chem. Soc.* **2006**, *128*, 14470.
(13) Marchetti, F.; Pinzino, C.; Zacchini, S.; Pampaloni, G. *Angew. Chem., Int. Ed.* **2010**, *49*, 5268.
(14) Chen, X.; Ma, B.; Wang, X.; Yao, S.; Ni, L.; Zhou, Z.; Li, Y.; Huang, W.; Ma, J.; Zuo, J.; Wang, X. *Chem. - Eur. J.* **2012**, *18*, 11828.
(15) Chen, X.; Ma, B.; Chen, S.; Li, Y.; Huang, W.; Ma, J.; Wang, X. *Chem. - Asian J.* **2013**, *8*, 238.
(16) Banerjee, M.; Lindeman, S. V.; Rathore, R. *J. Am. Chem. Soc.* **2007**, *129*, 8070.
(17) Banerjee, M.; Shukla, R.; Rathore, R. *J. Am. Chem. Soc.* **2009**, *131*, 1780.
(18) Scott, L. T. *Angew. Chem., Int. Ed.* **2003**, *42*, 4133.
(19) Kawase, T.; Kurata, H. *Chem. Rev.* **2006**, *106*, 5250.
(20) Tahara, K.; Tobe, Y. *Chem. Rev.* **2006**, *106*, 5274.
(21) Steinberg, B. D.; Scott, L. T. *Angew. Chem., Int. Ed.* **2009**, *48*, 5400.
(22) Eisenberg, D.; Shenhar, R.; Rabinovitz, M. *Chem. Soc. Rev.* **2010**, *39*, 2879.
(23) Iyoda, M.; Yamakawa, J.; Rahman, M. J. *Angew. Chem., Int. Ed.* **2011**, *50*, 10522.
(24) Evans, P. J.; Jasti, R. *Top. Curr. Chem.* **2013**, *4*, 1.
(25) Sisto, T. J.; Jasti, R. *Synlett* **2012**, *23*, 483.
(26) Hirst, E. S.; Jasti, R. *J. Org. Chem.* **2012**, *77*, 10473.
(27) Omachi, H.; Segawa, Y.; Itami, K. *Acc. Chem. Res.* **2012**, *45*, 1378.
(28) Yamago, S.; Kayahara, E.; Iwamoto, T. *Chem. Rec.* **2014**, *14*, 84.
(29) Golder, M. R.; Jasti, R. *Acc. Chem. Res.* **2015**, *48*, 557.
(30) Jasti, R.; Bhattacharjee, J.; Neaton, J. B.; Bertozzi, C. R. *J. Am. Chem. Soc.* **2008**, *130*, 17646.
(31) Sisto, T. J.; Golder, M. R.; Hirst, E. S.; Jasti, R. *J. Am. Chem. Soc.* **2011**, *133*, 15800.
(32) Darzi, E. R.; Sisto, T. J.; Jasti, R. *J. Org. Chem.* **2012**, *77*, 6624.
(33) Xia, J.; Bacon, J. W.; Jasti, R. *Chem. Sci.* **2012**, *3*, 3018.
(34) Xia, J.; Jasti, R. *Angew. Chem., Int. Ed.* **2012**, *51*, 2474.
(35) Evans, P. J.; Darzi, E. R.; Jasti, R. *Nat. Chem.* **2014**, *6*, 404.
(36) Takaba, H.; Omachi, H.; Yamamoto, Y.; Bouffard, J.; Itami, K. *Angew. Chem., Int. Ed.* **2009**, *48*, 6112.

DOI: 10.1021/jacs.5b10855
J. Am. Chem. Soc. 2016, 138, 338−344

(37) Omachi, H.; Matsuura, S.; Segawa, Y.; Itami, K. *Angew. Chem., Int. Ed.* **2010**, *49*, 10202.
(38) Segawa, Y.; Miyamoto, S.; Omachi, H.; Matsuura, S.; Šenel, P.; Sasamori, T.; Tokitoh, N.; Itami, K. *Angew. Chem., Int. Ed.* **2011**, *50*, 3244.
(39) Segawa, Y.; Šenel, P.; Matsuura, S.; Omachi, H.; Itami, K. *Chem. Lett.* **2011**, *40*, 423.
(40) Ishii, Y.; Nakanishi, Y.; Omachi, H.; Matsuura, S.; Matsui, K.; Shinohara, H.; Segawa, Y.; Itami, K. *Chem. Sci.* **2012**, *3*, 2340.
(41) Yamago, S.; Watanabe, Y.; Iwamoto, T. *Angew. Chem., Int. Ed.* **2010**, *49*, 757.
(42) Iwamoto, T.; Watanabe, Y.; Sakamoto, Y.; Suzuki, T.; Yamago, S. *J. Am. Chem. Soc.* **2011**, *133*, 8354.
(43) Kayahara, E.; Sakamoto, Y.; Suzuki, T.; Yamago, S. *Org. Lett.* **2012**, *14*, 3284.
(44) Kayahara, E.; Iwamoto, T.; Suzuki, T.; Yamago, S. *Chem. Lett.* **2013**, *42*, 621.
(45) Kayahara, E.; Patel, V. K.; Yamago, S. *J. Am. Chem. Soc.* **2014**, *136*, 2284.
(46) Patel, V. K.; Kayahara, E.; Yamago, S. *Chem. - Eur. J.* **2015**, *21*, 5742.
(47) Kayahara, E.; Patel, V. K.; Xia, J.; Jasti, R.; Yamago, S. *Synlett* **2015**, *26*, 1615.
(48) Xia, J.; Golder, M. R.; Foster, M. E.; Wong, B. M.; Jasti, R. *J. Am. Chem. Soc.* **2012**, *134*, 19709.
(49) Sisto, T. J.; Tian, X.; Jasti, R. *J. Org. Chem.* **2012**, *77*, 5857.
(50) Omachi, H.; Segawa, Y.; Itami, K. *Org. Lett.* **2011**, *13*, 2480.
(51) Yagi, A.; Segawa, Y.; Itami, K. *J. Am. Chem. Soc.* **2012**, *134*, 2962.
(52) Matsui, K.; Segawa, Y.; Itami, K. *Org. Lett.* **2012**, *14*, 1888.
(53) Matsui, K.; Segawa, Y.; Itami, K. *J. Am. Chem. Soc.* **2014**, *136*, 16452.
(54) Kubota, N.; Segawa, Y.; Itami, K. *J. Am. Chem. Soc.* **2015**, *137*, 1356.
(55) Kayahara, E.; Iwamoto, T.; Takaya, H.; Suzuki, T.; Fujitsuka, M.; Majima, T.; Yasuda, N.; Matsuyama, N.; Seki, S.; Yamago, S. *Nat. Commun.* **2013**, *4*, 2694.
(56) Iwamoto, T.; Kayahara, E.; Yasuda, N.; Suzuki, T.; Yamago, S. *Angew. Chem., Int. Ed.* **2014**, *53*, 6430.
(57) Kayahara, E.; Patel, V. K.; Mercier, A.; Kundig, E. P.; Yamago, S. *Angew. Chem., Int. Ed.* **2016**, *55*, 302.
(58) Kayahara, E.; Qu, R.; Kojima, M.; Iwamoto, T.; Suzuki, T.; Yamago, S. *Chem. - Eur. J.* **2015**, *21*, 18939.
(59) Hitosugi, S.; Nakanishi, W.; Yamasaki, T.; Isobe, H. *Nat. Commun.* **2011**, *2*, 492.
(60) Hitosugi, S.; Yamasaki, T.; Isobe, H. *J. Am. Chem. Soc.* **2012**, *134*, 12442.
(61) Nishiuchi, T.; Feng, X.; Enkelmann, V.; Wagner, M.; Müllen, K. *Chem. - Eur. J.* **2012**, *18*, 16621.
(62) Golling, F. E.; Quernheim, M.; Wagner, M.; Nishiuchi, T.; Müllen, K. *Angew. Chem., Int. Ed.* **2014**, *53*, 1525.
(63) Tran-Van, A.-F.; Huxol, E.; Basler, J. M.; Neuburger, M.; Adjizian, J.-J.; Ewels, C. P.; Wegner, H. A. *Org. Lett.* **2014**, *16*, 1594.
(64) Huang, C.; Huang, Y.; Akhmedov, N. G.; Popp, B. V.; Petersen, J. L.; Wang, K. K. *Org. Lett.* **2014**, *16*, 2672.
(65) Jiang, H.-W.; Tanaka, T.; Mori, H.; Park, K. H.; Kim, D.; Osuka, A. *J. Am. Chem. Soc.* **2015**, *137*, 2219.
(66) Ball, M.; Fowler, B.; Li, P.; Joyce, L. A.; Li, F.; Liu, T.; Paley, D.; Zhong, Y.; Li, H.; Xiao, S.; Ng, F.; Steigerwald, M. L.; Nuckolls, C. *J. Am. Chem. Soc.* **2015**, *137*, 9982.
(67) Chen, Q.; Trinh, M. T.; Paley, D. W.; Preefer, M. B.; Zhu, H.; Fowler, B. S.; Zhu, X. Y.; Steigerwald, M. L.; Nuckolls, C. *J. Am. Chem. Soc.* **2015**, *137*, 12282.
(68) Kayahara, E.; Kouyama, T.; Kato, T.; Takaya, H.; Yasuda, N.; Yamago, S. *Angew. Chem., Int. Ed.* **2013**, *52*, 13722.
(69) Zabula, A. V.; Filatov, A. S.; Xia, J.; Jasti, R.; Petrukhina, M. A. *Angew. Chem., Int. Ed.* **2013**, *52*, 5033.
(70) Fujitsuka, M.; Tojo, S.; Iwamoto, T.; Kayahara, E.; Yamago, S.; Majima, T. *J. Phys. Chem. Lett.* **2014**, *5*, 2302.
(71) Toriumi, N.; Muranaka, A.; Kayahara, E.; Yamago, S.; Uchiyama, M. *J. Am. Chem. Soc.* **2015**, *137*, 82.
(72) Talipov, M. R.; Jasti, R.; Rathore, R. *J. Am. Chem. Soc.* **2015**, *137*, 14999.
(73) Segawa, Y.; Fukazawa, A.; Matsuura, S.; Omachi, H.; Yamaguchi, S.; Irle, S.; Itami, K. *Org. Biomol. Chem.* **2012**, *10*, 5979.
(74) Nishihara, T.; Segawa, Y.; Itami, K.; Kanemitsu, Y. *J. Phys. Chem. Lett.* **2012**, *3*, 3125.
(75) Fujitsuka, M.; Iwamoto, T.; Kayahara, E.; Yamago, S.; Majima, T. *ChemPhysChem* **2013**, *14*, 1570.
(76) Alvarez, M. P.; Burrezo, P. M.; Kertesz, M.; Iwamoto, T.; Yamago, S.; Xia, J.; Jasti, R.; Navarrete, J. T. L.; Taravillo, M.; Baonza, V. G.; Casado, J. *Angew. Chem., Int. Ed.* **2014**, *53*, 7033.
(77) Fujitsuka, M.; Lu, C.; Iwamoto, T.; Kayahara, E.; Yamago, S.; Majima, T. *J. Phys. Chem. A* **2014**, *118*, 4527.
(78) Pena Alvarez, M.; Mayorga Burrezo, P.; Iwamoto, T.; Qiu, L.; Kertesz, M.; Taravillo, M.; Baonza, V. G.; Lopez Navarrete, J. T.; Yamago, S.; Casado, J. *Faraday Discuss.* **2014**, *173*, 157.
(79) Chen, H.; Golder, M. R.; Wang, F.; Jasti, R.; Swan, A. K. *Carbon* **2014**, *67*, 203.
(80) Hines, D. A.; Darzi, E. R.; Jasti, R.; Kamat, P. V. *J. Phys. Chem. A* **2014**, *118*, 1595.
(81) Iwamoto, T.; Watanabe, Y.; Sadahiro, T.; Haino, T.; Yamago, S. *Angew. Chem., Int. Ed.* **2011**, *50*, 8342.
(82) Iwamoto, T.; Watanabe, Y.; Takaya, H.; Haino, T.; Yasuda, N.; Yamago, S. *Chem. - Eur. J.* **2013**, *19*, 14061.
(83) Iwamoto, T.; Slanina, Z.; Mizorogi, N.; Guo, J.; Akasaka, T.; Nagase, S.; Takaya, H.; Yasuda, N.; Kato, T.; Yamago, S. *Chem. - Eur. J.* **2014**, *20*, 14403.
(84) Nakanishi, Y.; Omachi, H.; Matsuura, S.; Miyata, Y.; Kitaura, R.; Segawa, Y.; Itami, K.; Shinohara, H. *Angew. Chem., Int. Ed.* **2014**, *53*, 3102.
(85) Ueno, H.; Nishihara, T.; Segawa, Y.; Itami, K. *Angew. Chem., Int. Ed.* **2015**, *54*, 3707.
(86) Connelly, N. G.; Geiger, W. E. *Chem. Rev.* **1996**, *96*, 877.
(87) Stone, A. J. *Proc. R. Soc. London, Ser. A* **1963**, *271*, 424.
(88) Stone, A. J. *Mol. Phys.* **1963**, *6*, 509.
(89) Stone, A. J. *Mol. Phys.* **1964**, *7*, 311.

DOI: 10.1021/jacs.5b10855
J. Am. Chem. Soc. 2016, 138, 338−344